

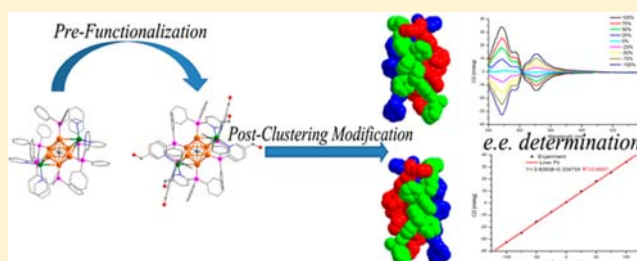
Postclustering Dynamic Covalent Modification for Chirality Control and Chiral Sensing

Yang Yang, Xiao-Li Pei, and Quan-Ming Wang*

State Key Lab of Physical Chemistry of Solid Surfaces Department of Chemistry, College of Chemistry and Chemical Engineering, Xiamen University, Xiamen, Fujian, People's Republic of China

S Supporting Information

ABSTRACT: Cluster-based functional materials are appealing, because clusters are well-defined building units that can be rationally incorporated for the tuning of structures and properties. Postclustering modification (PCM) allows for tailoring properties through the structural modification of a cluster with preorganized functional groups. By introducing aldehydes into a robust gold–silver cluster via a protection–deprotection process, we manage to synthesize a new cluster bearing six reactive sites, which are available for PCM through dynamic covalent imine bonds formation with chiral monoamines. Chirality is transferred from the amine to the gold–silver cluster. The homochirality of the resulted cluster has been confirmed by X-ray structural determination and CD spectroscopy. Intense CD signals make it practical for chiral recognition and *ee* value determination of chiral monoamines. The strategy of prefunctionalizing of cluster and the concept of PCM open a broader prospect for cluster design and applications.



INTRODUCTION

Metal cluster compounds (“clusters” in short hereafter) comprise multicomponents including many metal centers and organic ligands. They display interesting properties due to the collective effect integrated from the subunits.^{1–6} Great effort has been made to tune the properties of a cluster by dealing with either the cluster core^{7–9} or ligands.^{6,10–14} Postsynthetic modification method has been extensively applied in diversification of metal–organic frameworks^{15–17} and post-self-assembly approach has provided an alternative means to conventional coordination-driven self-assembly.^{18–20} Furthermore, the reactivities of monolayer protected clusters have been investigated through synthetic transformation of the ligand sphere.^{6,10–14} We are especially interested in cluster-based materials, because their well-defined composition and structures are helpful for elucidating structure–property relationships, which are important in the development of new cluster systems of various potential applications. To this end, we have initiated a strategy to preorganize organic functional groups in a structurally well-defined cluster, and applied “dynamic covalent chemistry” principle in subsequent covalent modification of clusters.^{21,22}

Clusters suitable for postclustering covalent modification (PCM) should be robust both in the preorganizing and postclustering processes. A good candidate is $[\text{Au}_6\text{Ag}_2(\text{C})(\text{dppy})_6](\text{BF}_4)_4$ (dppy = diphenylphosphino-2-pyridine) (**A**, Figure 1a).⁷ First, this cluster is very stable, and it remains intact even under the treatment of potassium permanganate in boiling MeCN for 2 days. Moreover, it bears aromatic chromophores and has excellent optical properties. Finally, it

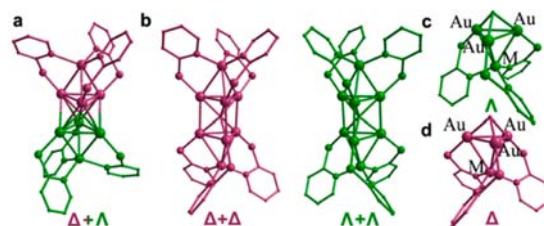


Figure 1. (a) Structure of **A** with $\Delta+\Lambda$ silver centers ($M = \text{Ag}$). (b) Structure of **B** with $\Delta+\Delta$ (left) or $\Lambda+\Lambda$ (right) copper centers ($M = \text{Cu}$). (c) **C**: Λ configuration of Au_3M moiety. (d) **D**: Δ configuration. Phenyl groups, hydrogen atoms, and counterions are omitted for clarity.

contains novel stereodynamic components available for chirality control, which may have potential applications in chiral sensing.²³

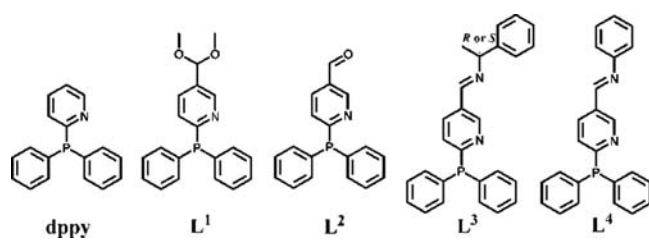
Cluster **A** has a bicapped octahedral configuration (Figure 1a), and its copper analogue $[\text{Au}_6\text{Cu}_2(\text{C})(\text{dppy})_6](\text{BF}_4)_4$ (**B**, an enantiomeric pair, Figure 1b) is a bicapped trigonal prism.²⁴ These two structures each could be viewed as the fusion of two Au_3M ($M = \text{Ag}, \text{Cu}$) moieties (**C** or **D**, Figure 1c,d) sharing a carbon center but in different ways. The silver or copper atom locks the conformation of the aryl rings. Pyridyl groups of dppy ligands wrap M with the $M\text{--}N$ coordinating bonds to form a triblade propeller configuration, which is a chiral moiety (Δ or Λ) as shown in Figure 1c,d. The bicapped trigonal prismatic **B**

Received: July 22, 2013

Published: September 30, 2013

is chiral, as Au_3Cu moieties of the same handedness join together ($\Lambda+\Lambda$ or $\Delta+\Delta$, Figure 1b). However, equal amount $\Lambda+\Lambda$ and $\Delta+\Delta$ clusters are present in the crystal to give a racemic mixture. On the contrary, the bicapped octahedral **A** is achiral, which is generated from two Au_3Ag units of opposite conformations ($\Delta+\Lambda$, Figure 1a). As a result, **A** is centrosymmetric and may be regarded as a *meso* compound. DFT calculation suggests that the energy difference between the octahedral and trigonal prismatic cores is small,²⁴ so the configurations of **A** and **B** can be interconverted through the relative rotation (60 deg) of the upper and lower moieties along with a chiral inversion of one of the *M* centers. External factors are necessary for the chirality control in these stereodynamic CAu_6M_2 systems, and PCM is a convenient approach for introducing chiral factors.

Chart 1. Structures of Phosphine Ligands



In this article, we describe our attempt to preorganize aldehyde groups to **A** using an aldehyde protection–deprotection approach, which leads to the formation of $[Au_6Ag_2(C)(L^2)_6](BF_4)_4$ (**1**, $L^2 = 2$ -(diphenylphosphino)-5-pyridinecarboxaldehyde). Chirality control was realized via PCM with α -chiral monoamines to generate homochiral cluster $[Au_6Ag_2(C)(L^3)_6](BF_4)_4$ (**4a** *S* α -chiral monoamines or **4b** *R* α -chiral monoamines). CD spectroscopy was utilized to determine the absolute configurations of the clusters. We will

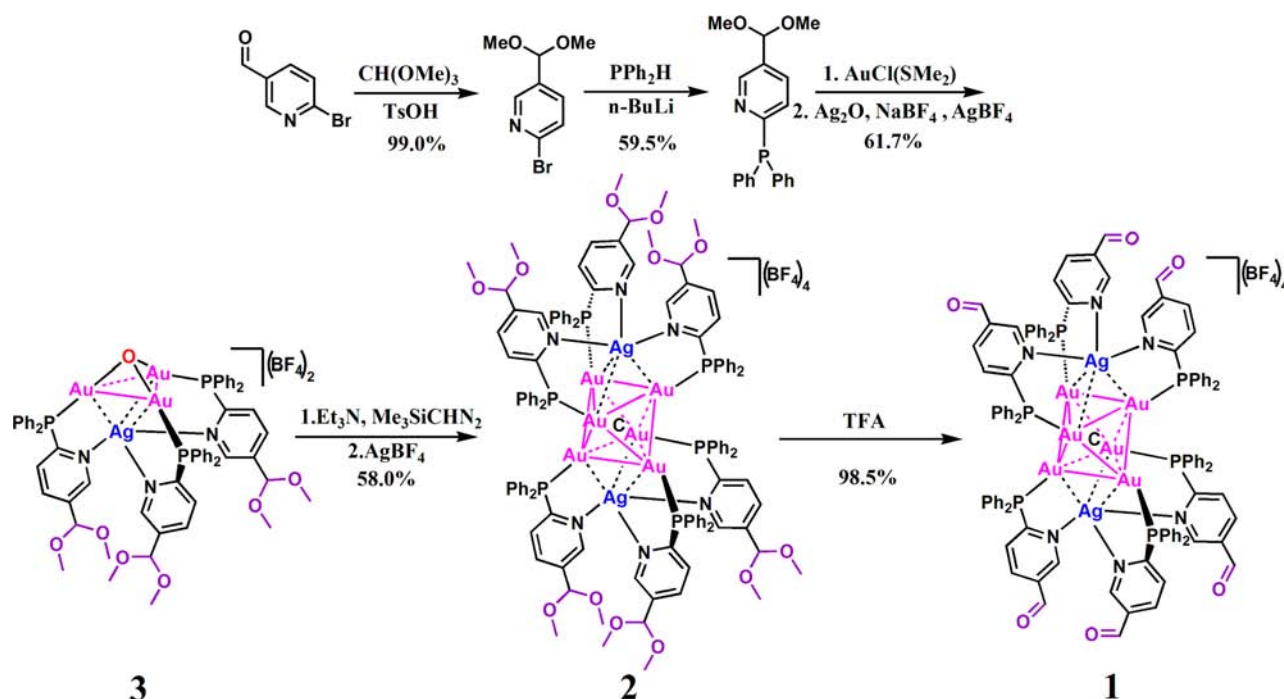
also show that the PCM approach is of practical use in the convenient determination of *ee* values of α -chiral monoamines.

RESULTS AND DISCUSSION

The synthesis is outlined in Scheme 1. The preparation of **1** bearing hexa-aldehyde needs a protection of the aldehyde groups, because the direct use of L^2 , a phosphine containing aldehyde group, caused redox reactions between aldehydes and $Au(I)$ or Ag_2O in the preparation of gold(I)–silver(I) clusters. To preorganize aldehyde groups in a cluster, we used a protection–deprotection strategy, i.e. the aldehyde was protected by transforming aldehyde groups into acetals with methanol.²⁵ As a result, ligand L^1 (2-(diphenylphosphino)-5-(dimethoxymethyl)pyridine), the protected form of L^2 , was employed at the beginning of the synthesis as shown in Scheme 1. The precursor $[Au_3Ag(O)(L^1)_3](BF_4)_2$ (**3**, Figure 2a) is an oxo cluster which was prepared through the treatment of $Au(L^1)Cl$ with Ag_2O in acetone. The reaction of **3** with Me_3SiCHN_2 (trimethylsilyldiazomethane) gave robust carbon-centered cluster $[Au_6Ag_2(C)(L^1)_6](BF_4)_4$ (**2**, Figure 2b). Aldehyde groups were recovered through hydrolysis of **2** in trifluoroacetic acid (TFA). As a result, **2** was transformed to **1** that is a key cluster for further covalent modification.

The identities of **1–3** have been confirmed by microanalysis, spectroscopy, and single crystal structural analysis.²⁶ Yellow crystals of **1** were grown by layering diethyl ether onto the filtrate of the reaction mixture in TFA and CH_2Cl_2 solution. Cluster **1** has a bicapped octahedral CAu_6Ag_2 core with six aldehydes attached, which is similar to **A** (Figure 2c). The 1H NMR and IR spectra of **1** show unambiguously the presence of aldehyde groups. A sharp singlet in ^{31}P NMR spectrum and only one set 1H NMR signals of the phosphine ligands are consistent with the high symmetry of **1**. ESI mass spectrometry confirmed the presence of molecular ion $[Au_6Ag_2(C)(L^2)_6]^{4+}$ with a $m/z = 789.288$ (calcd 789.024) in solution. The isotopic pattern matches perfectly the simulated one (Figure S23,

Scheme 1. Synthetic Route of **1** Containing Preorganized Hexa-Aldehyde



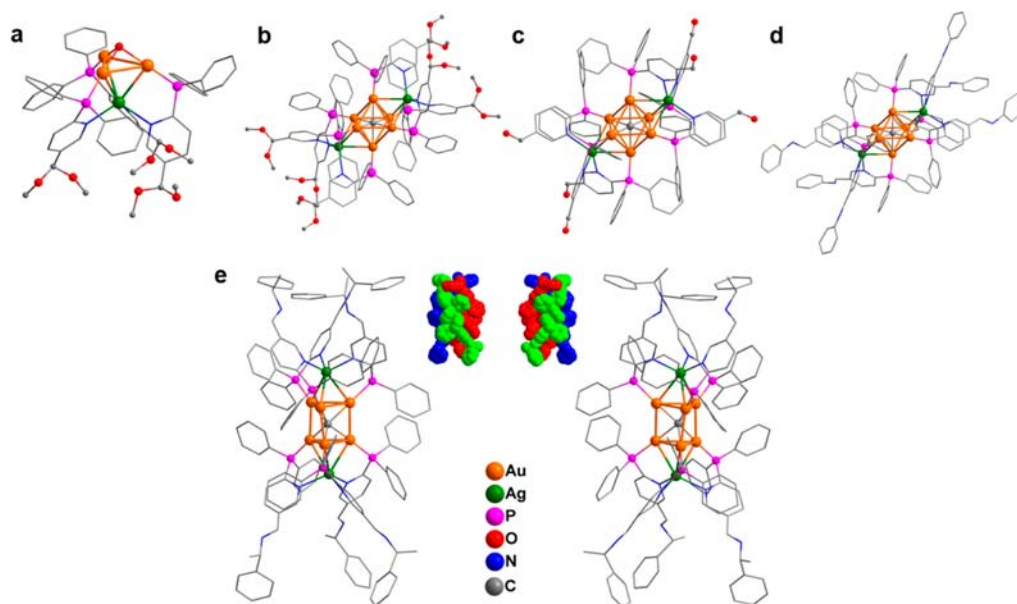


Figure 2. Molecular structures of the cation part of (a) **3**, (b) **2**, (c) **1**, (d) **5**, (e) **4a** (left) and **4b** (right); inset: space-filling models of **4a** (left) and **4b** (right). Hydrogen atoms have been omitted for clarity.

Supporting Information), which indicates **1** stays intact in solution.

Chirality control was performed through PCM of **1** (Figure 3a). The coupling of aldehyde groups of **1** with chiral amines led to the formation of imine bonds, as a result chiral clusters were formed. When **1** reacted with *S*-1-phenylethylamine in acetonitrile, **4a** [$\text{Au}_6\text{Ag}_2(\text{C})(\text{S-L}^3)_6(\text{BF}_4)_4$] was isolated in high yield. The aldehyde peak almost disappeared in ^1H NMR spectrum of **4a** in comparison to **1**, and signals from protons of $-\text{NH}_2$ were not observable. In IR spectrum of **4a**, $\text{C}=\text{O}$

vibration peak at 1707 cm^{-1} is replaced by $\text{C}=\text{N}$ vibration band at 1638 cm^{-1} . ESI-MS analysis also confirms the existence of **4a** in solution. (Figure S22, Supporting Information)

Red crystals of **4a** were grown by diffusing diethyl ether into its dichloromethane solution. Cluster **4a** crystallizes in chiral space group $R32$. The cluster core is a slightly distorted bicapped trigonal prism (Figure 2e left), which is similar to that in **B**. The $\text{Au}\cdots\text{Au}$ and $\text{Au}\cdots\text{Ag}$ distances vary from $2.741(1)$ to $2.915(2)$ Å, suggesting the presence of metallophilic interactions. The $\text{Au}\cdots\text{Au}$ distance is also comparable with those of **B**. A carbon tetraanion is located at the center of the Au_6Ag_2 core with $\text{Au}-\text{C}$ lengths in the range $2.15(2)$ – $2.18(2)$ Å. A C_3 symmetry axis passes through the line $\text{Ag}1\cdots\text{C}\cdots\text{Ag}2$ with the $\text{Ag}1\cdots\text{Ag}2$ separation of 7.440 Å. In comparison with **A**, the trigonal prismatic core is stabilized by shorter $\text{Au}\cdots\text{Au}$ contacts and intramolecular $\pi\cdots\pi$ interactions between the phenyl moieties of neighboring L^3 ligands, with the centroid to centroid distance between the aryl rings being 3.86 Å. Each cluster is covalently connected with six chiral amines through imine bonds, and the cluster is homochiral as the chiral amines disrupt any center or plane of symmetry. In a Au_3Ag moiety, three L^3 ligands each is coordinated to a gold(I) atom with the P donor, and the three pyridyl groups are bound to the silver(I) atom in the way like a triblade propeller of 3 symmetry. The dihedral angle between the adjacent pyridyl groups is about 88.8° . Both Ag^{I} centers adopt identical conformation ($\Lambda+\Lambda$), resulting in a chiral *M* helical molecule. All molecules in the crystal are homochiral. The absolute configuration and enantiopurity were supported by the Flack factor $-0.02(3)$. When a similar PCM procedure was taken with *R*-1-phenylethylamine, [$\text{Au}_6\text{Ag}_2(\text{C})(\text{R-L}^3)_6(\text{BF}_4)_4$] (**4b**, Figure 2e right) was formed and isolated. Structural determination shows that **4b** is the enantiomer of **4a**. Cluster **4b** is a *P* helicate with two Ag^{I} centers in Δ conformation ($\Delta+\Delta$). This clearly demonstrated that the cluster chirality was dictated by the absolute configuration of the chiral amine used in the reaction.

The condensation between **1** and chiral amine causes a dramatic change of the cluster core configuration, i.e. an octahedron in achiral **1** was changed to a trigonal prism in

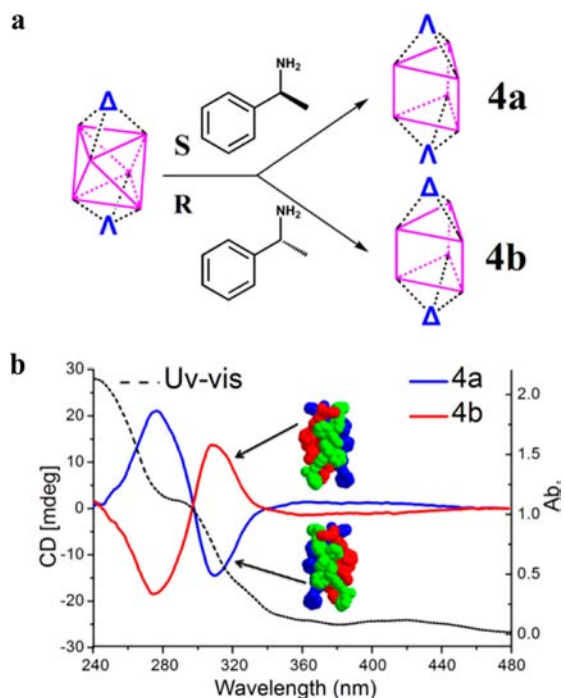


Figure 3. (a) Schematic illustration of the chirality control. (b) CD spectra of enantiomers **4a** (blue trace) and **4b** (red trace), and UV-vis spectrum of **4a** (dotted line) in dichloromethane (DCM).

chiral **4**. A given chiral amine promotes a specific configuration of the Au_3M moiety like other triblade propeller systems.^{27–30} Both Au_3M moieties have to adopt the same configuration due to the same chirality transferred from the amine, which requires the transformation of the core. Molecular simulation study revealed that homochiral bicapped octahedron ($\Lambda+\Lambda$ or $\Delta+\Delta$) and heterochiral bicapped trigonal prism ($\Delta+\Lambda$) are not favorable due to serious steric hindrance between the phenyl groups of dppy ligands from different Au_3M moieties (Figures S26 and S27, Supporting Information). Consequently, homochiral $\text{Au}_6\text{M}_2\text{C}$ prefers the bicapped trigonal prismatic structure. Thus there is a strong diastereoselectivity during the formation of **4a** and **4b** when PCM is done with a chiral amine. The stereodynamic nature of the $\text{Au}_6\text{M}_2\text{C}$ systems is critical for the structural transformation. Molecular structures of **4a** and **4b** presented here represent valuable structural evidence that a gold cluster core is sensitive to the chiral environment.^{31–33}

The important roles played by chiral amines were also verified by the use of an achiral amine as the control. The reaction between **1** and aniline resulted in the formation of an achiral cluster $[\text{Au}_6\text{Ag}_2(\text{C})(\text{L}^+)]_6(\text{BF}_4)_4$ (**5**, Figure 2d). X-ray structural analysis indicated that **5** is a centrosymmetric bicapped octahedral cluster consisting of both Δ and Λ Au_3Ag units, which is silent in circular dichroism (CD) spectroscopy. Our attempt to crystallize the condensation product using benzylamine as a control was unsuccessful.

Interestingly, the cluster core configurations are related to the color of their crystals. Octahedral clusters (**A**, **1**, **2**, **5**) are yellow while trigonal prismatic clusters (**B**, **4a**, **4b**) are red. Since the only difference between these two types of clusters is the pattern of gold(I)–gold(I) contacts, twelve longer $\text{Au}^1\cdots\text{Au}^1$ contacts in a octahedral Au_6 versus nine shorter $\text{Au}^1\cdots\text{Au}^1$ contacts in a trigonal prismatic Au_6 cluster-based electronic transitions account for the color difference.

The enantiomeric relationship between **4a** and **4b** is supported by CD spectroscopy. Their CD spectra in dichloromethane showed perfect mirror image with respect to each other (Figure 3b). Moreover, the intense CD signals also indicated that **4a** and **4b** reserve their bicapped trigonal prismatic configuration in solution. Otherwise the octahedral cluster would not give such intense induced CD signals. The bisignate signals of the CD bands around 255–345 nm arise from the exciton coupling of ligand centered $\pi-\pi^*$ transitions. The nulls of the CD signals at 297 nm are exactly the absorption shoulder position in the UV–vis spectrum, which is consistent with exciton coupling theory.^{27,34–36} Interestingly, internuclear coupling effects were observed.³⁷ For example, **4a** has $\Lambda+\Lambda$ absolute configuration, but it displays a negative exciton couplet in the CD spectrum, which conflicts the prediction of exciton theory, i.e. positive sign should be observed corresponding to a Λ configuration as predicted for mononuclear chiral center. These data indicate that internuclear excitation coupling happens between the two Λ chiral units. **4b** also shows such an “anomalous” CD spectrum.^{37–39}

Once chiral amines are covalently attached to **1**, the chirality of the amines dictates the configuration of the cluster. Due to the dynamic nature of imine bonds, amine exchange occurs readily when another amine with the opposite chirality is added. The cluster cannot withstand the chiral influence from the opposite handedness of the new coming amines, so the chirality of the cluster will be inverted.⁴⁰ This is confirmed by monitoring the CD signals of the reaction mixture, e.g. the

CD image of **4b** can be inverted by adding 10-fold excess of *S*-1-phenylethylamine into its acetonitrile solution through amines exchange reaction (Figure 4). The asymmetry of the spectrum is due to the excess *S*-1-phenylethylamine that is weak CD active.

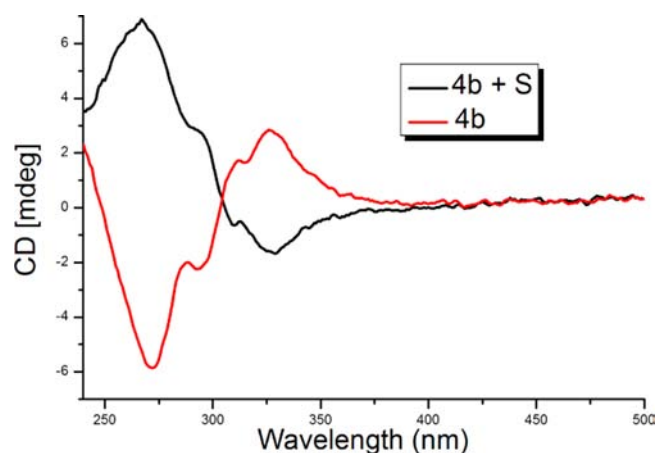


Figure 4. Inversion of CD signal of **4b** via amine exchange by reacting **4b** with 10-fold excess of *S*-1-phenylethylamine for 24 h in MeCN. For CD analysis, samples were diluted to 2.5×10^{-6} M.

Of special interest, cluster **1** can be used as a sensing probe to determine the absolute configurations and *ee* values of α -chiral amines, which are useful building units for the synthesis of pharmaceutical and agricultural target products.^{41,42} The efficient and accurate determination of the *ee* values of α -chiral amines can be done with CD as a chiroptical method for stereochemical analysis, which costs much less labor and time compared with HPLC etc.^{23,43,44} α -Chiral amines lacking strong chromophores can be conjugated to **1** via imine bonds, and the chirality of amines could be transferred to **1** that possesses stereochemically labile chromophoric moieties.

Six α -chiral monoamines including aliphatic and aromatic ones (Figure 5a) were used as model compounds for *in situ* chirality checking with **1**. Typically, six equivalent amount of an amine was mixed with **1** in acetonitrile solution, and then CD spectra were measured directly after the condensation finished. No workup is needed. Taking *S*-1-phenylethylamine as an example, intense induced CD signals could be detected in the range of 245–375 nm in the course of its condensation with **1** (Figure 5b). The condensation finished in 50 min with CD signal at 271 nm reached its maximum intensity (Figure S29). The CD spectrum of the condensation product between *S*-1-phenylethylamines and **1** has the same profile as that measured from MeCN solution of crystals of **4a**. Pure chiral amines showed much weaker signals at shorter wavelengths, and simple mixing formylpyridine with the chiral amine did not improve. This observation indicates the importance of the chromophores while **1** was transformed to **4a**. *R*-Amines resulted in the observation of a negative Cotton effect at 271 nm, while the *S*-amines give opposite signals. It is noteworthy that although it took 50 min for the reaction to finish, the signal of the CD spectrum is significant enough for chiral recognition in 10 min.

To evaluate the practical application of **1** in quantitative *ee* determination, we use 1-phenylethylamine as a model analyte. A series of 1-phenylethylamine samples with different *ee* values of the same concentration were prepared for calibration curve construction. Each condensation reaction was conducted with

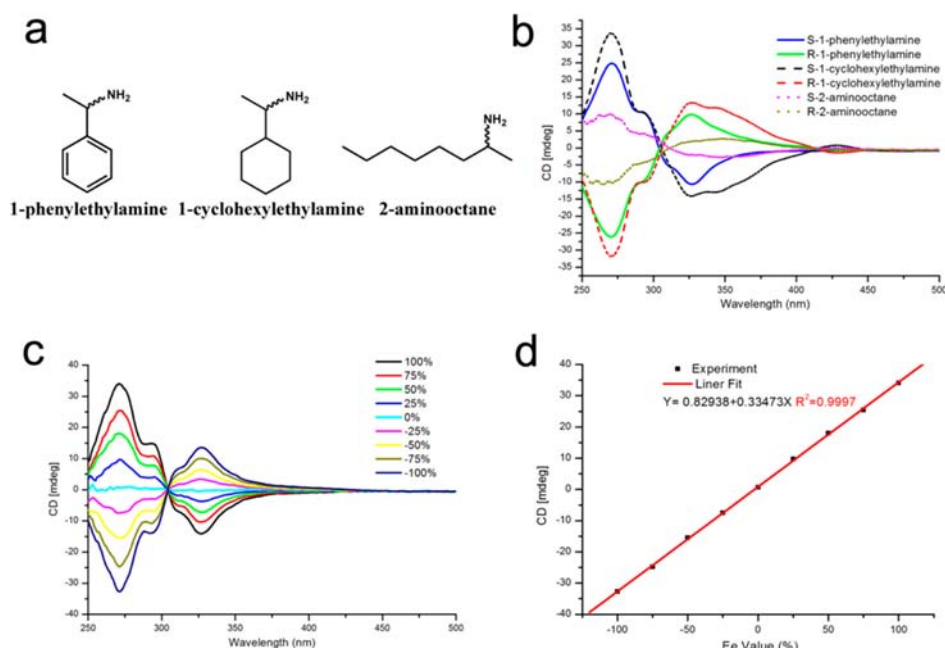


Figure 5. (a) Six model aliphatic and aromatic α -chiral monoamines. (b) CD spectra of the reaction mixture of **1** and the six model chiral monoamines in MeCN. (c) CD spectra of the reaction mixture of varied *ee* value of 1-phenylethylamine and **1** in MeCN (pure *S*-1-phenylethylamine regarded as *ee* = 100%, and pure *R*-1-phenylethylamine regarded as *ee* = -100%). (d) Calibration curve by plotting CD readings at 271 nm in Figure 5c against *ee* values of chiral 1-phenylethylamine.

the concentration of **1** at 4.76×10^{-4} M, then a 100 μ L sample solution was diluted to 1.54×10^{-5} M for CD analysis. The plot of CD intensities at 271 nm against *ee* values shows an excellent linear relationship with $R^2 = 0.9997$ (Figure 5d). Eight representative samples covering a wide range of *ee* values were used to test the determination accuracy. The measured results are quite close to the actual values with absolute errors less than 2.5%, which were derived from the linear regression equation and CD readings at 271 nm as shown in Table 1. Cluster **1** also performed well in the *ee* values determination of cyclic 1-cyclohexylethylamine and aliphatic 2-amino-octane (Table 1) with linear calibration curves (Figures S33 and S36, Supporting Information). The largest absolute errors are 2.0% and 5.9% for 1-cyclohexylethylamine and 2-amino-octane, respectively. Regarding the determination of *ee* values of amines, Anslyn et al. have developed a rapid method by *in situ* assembly of octahedral Fe(II) complexes for chiral monoamine,²⁷ and Wolf et al. designed a stereodynamic organic framework for chiral diamines sensing.⁴⁵ Our method presents an advantageous alternative with good linear calibration curve, which is useful for quantitative *ee* analysis with high accuracy. An additional advantage is that cluster **1** could be recovered by treating with TFA. After hydrolysis diethyl ether was added to precipitate a solid of cluster **1**, which was recrystallized in TFA and dichloromethane to give pure **1** in 80% yield (see Supporting Information).

CONCLUSION

In this paper, we have made a successful attempt to perform prefunctionalization and postclustering modification of well-defined clusters. The incorporation of aldehyde groups into achiral bicapped octahedral cluster **A** through protection–deprotection process led to the formation of **1** bearing reactive sites available for PCM with chiral amines. The induced chirality of the cluster is dictated by chiral amine pendants, as a

Table 1. Determination of the *ee* Values of 1-Phenylethylamine, 1-Cyclohexylethylamine, and 2-Amino-octane

analyte	actual <i>ee</i> (%)	calcd <i>ee</i> (%)	absolute error (%)
1-phenylethylamine	80.0	80.0	0.0
	60.0	58.7	1.3
	30.0	29.5	0.5
	10.0	10.7	0.7
	-20.0	-22.5	2.5
	-40.0	-41.3	1.3
	-66.7	-67.0	0.3
	-85.0	-85.6	0.3
1-cyclohexylethylamine	86.7	87.8	1.1
	66.7	66.0	0.7
	33.3	35.1	1.8
	20.0	22.0	2.0
	10.0	9.8	0.2
	-15.0	-15.6	0.6
	-40.0	-39.8	0.2
	-70.0	-71.3	1.3
2-amino-octane	10.0	7.4	2.6
	30.0	27.4	2.6
	60.0	57.6	2.4
	85.0	90.1	5.1
	-15.0	-16.4	1.4
	-40.0	-38.8	1.2
	-70.0	-75.9	5.9
	-91.7	-93.2	1.5

result of the transformation of the stereodynamic gold–silver cluster from an achiral octahedron into a chiral trigonal prism. The process is stereospecific with a chiral amine promoting one absolute configuration of bicapped trigonal prismatic cluster over the other. Structural evidence and CD data indicate that the gold cluster core is sensitive to chiral environments.

Inspiringly, strong induced CD signals generated from the chirality transfer from chiral amines to gold–silver clusters allow for rapid determination of α -chiral amine configurations and accurate measurement of the *e.e.* values of α -chiral amines. We believe that cluster **1** will be useful in various applications because its six aldehyde groups enable the incorporation of diverse substrates through PCM.

EXPERIMENTAL SECTION

All reagents employed were commercially available and used without further purification. The solvents used were of analytical grade. Silver tetrafluoroborate and the chiral amines were obtained from J&K Chemical. The ligand **L**¹ was prepared in a synthetic procedure similar to that of the literature method.²⁵ [O(AuL¹)₃Ag](BF₄)₂ (**3**) and [C(AuL¹)₆Ag₂](BF₄)₄ (**2**) were prepared according to literature method.⁷

2-Bromo-5-(dimethoxymethyl)pyridine. 2-Bromo-5-formylpyridine (10 g, 54.2 mmol), *p*-toluenesulphonic acid (204 mg, cat.), and trimethylorthoformate (25 mL) were added to a flask and sparged with nitrogen. After 100 mL dry methanol was injected with syringe, the mixture was refluxed at 68 °C for 4 h. The solution was cooled down to room temperature, 80 mL of dichloromethane was added, and the mixture was washed with sat. Na₂CO₃ and water. The aqueous layers were extracted with dichloromethane. The combined organic solution was washed with brine, dried with MgSO₄, and finally evaporated to yield a yellow oil (12.4 g, 99.0%). ¹H NMR (400.1 MHz; CDCl₃; ppm): δ 8.43 (d, *J* = 2.4 Hz, *H* = 1, 6-py), 7.64 (dd, *J*₁ = 8.4 Hz, *J*₂ = 2.4 Hz, *H* = 1, 3-py), 7.50 (d, *J* = 8.4 Hz, *H* = 1, 4-py), 5.43 (s, *H* = 1, CH(OMe)₂), 3.30 (s, *H* = 6, -OMe). ¹³C NMR (100.6 MHz, CDCl₃, ppm): 149.00 (s), 142.06 (s), 137.17 (s), 133.07 (s), 127.63 (s), 100.48 (s), 52.54 (s).

L¹: 2-(Diphenylphosphino)-5-(dimethoxymethyl)-pyridine. A solution of diphenylphosphine (6.0 mL, 34.6 mmol) in dry THF (40 mL) was cooled to 0 °C in ice water bath. *n*-BuLi (21.6 mL, 1.6 M in hexanes, 34.6 mmol) was injected dropwise over 15 min. The resulted solution was stirred in the bath for 90 min to give a dark red solution. To another flask sparged with nitrogen were added 2-bromo-4-(dimethoxymethyl)pyridine (8.0 g, 34.5 mmol) and THF (40 mL). Both flasks were cooled to -78 °C. The solution of 2-bromo-4-(dimethoxymethyl)pyridine was slowly injected into the PPh₂Li solution. The reaction mixture was further stirred overnight and allowed to warm to room temperature. All next workup was operated with deoxygenated solvents under nitrogen atmosphere. The reaction was stopped by adding water and diethyl ether. The aqueous layer was separated and back extracted with diethyl ether. The combined organic layers were washed with brine and dried with Na₂SO₄. The final solution was concentrated under reduced pressure to give the crude product, which was purified by flash column chromatography on silica gel (15:85 ethyl acetate:hexane) to afford a slightly yellow oil (6.91 g 69.5%). ¹H NMR (400.1 MHz, CDCl₃, ppm): δ 8.80 (d, *J*_{H-P} = 1.6 Hz, *H* = 1, 6-py), 7.63 (dt, *J*_{H-H} = 8.0 Hz, *J*_{H-P} = 1.6 Hz, *H* = 1, 3-py), 7.36–7.43 (m, *H* = 4, *o*-Ph₂), 7.27–7.35 (m, *H* = 6, *m*, *p*-Ph₂), 7.10 (d, *J*_{H-H} = 8.0 Hz, *H* = 1, 4-py), 5.42 (s, *H* = 1, CH(OMe)₂), 3.31 (s, *H* = 6, -OMe). ¹³C NMR (100.6 MHz, CDCl₃, ppm): δ 164.23 (d, *J*_{C-P} = 3.6 Hz), 149.15 (d, *J*_{C-P} = 13.0 Hz), 136.18 (d, *J*_{C-P} = 10.9 Hz), 134.24 (d, *J*_{C-P} = 2.4 Hz), 134.21 (d, *J*_{C-P} = 19.9 Hz), 132.18, 129.10, 128.69 (d, *J*_{C-P} = 7.4 Hz), 127.33 (d, *J*_{C-P} = 15.9 Hz), 101.31, 52.71. ³¹P NMR (162 MHz, CDCl₃, ppm): δ -2.46 (s). FT-ICR-MS (MeCN) calculated for C₂₀H₂₁NO₂P [MH]⁺, *m/z* = 338.130; found *m/z* = 338.130.

3: [Au₃Ag₁(O)(L¹)₃](BF₄)₂. To a solution of L¹ (400 mg, 1.19 mmol) in CH₂Cl₂ (30 mL) was added Au(Me₂S)Cl (350 mg, 1.19 mmol). After being stirred for 20 min, the solution was evaporated to dryness to afford a white solid. The white solid was then dissolved in 60 mL acetone. Freshly prepared Ag₂O (605 mg, 2.61 mmol) was added into the above solution, followed by NaBF₄ (746 mg 6.78 mmol) and AgBF₄ (232 mg, 1.19 mmol). The mixture was stirred for 3 h in the absence of light before the acetone was removed. The solid residue was extracted with CH₂Cl₂ (3 × 20 mL). The combined

extract was concentrated to dark brown oil under reduced pressure, which was triturated with diethyl ether to afford a dark brown solid (464 mg, 61.7%). ¹H NMR (400.1 MHz, CD₂Cl₂, ppm): δ 7.91 (d, *J*_{H-H} = 8.0 Hz, *H* = 3, 4-py), 7.76 (s, *H* = 3, 6-py), 7.26–7.58 (m, *H* = 3, Ph and 4-py), 5.12 (s, *H* = 3, CH(OMe)₂), 3.19 (s, *H* = 18, -OMe). ¹³C NMR (100.6 MHz, CD₂Cl₂, ppm): δ 152.11 (d, *J*_{C-P} = 112.0 Hz), 151.03 (d, *J*_{C-P} = 17.1 Hz), 138.51, 138.02 (broad), 134.26 (d, *J*_{C-P} = 14.1 Hz), 133.52, 120.19, 129.98 (d, *J*_{C-P} = 12.1 Hz), 124.63 (d, *J*_{C-P} = 61.4 Hz), 100.20, 53.76. ³¹P NMR (162 MHz, CD₂Cl₂, ppm): δ 29.46 (s). Anal. Calcd. for C₆₀H₆₀B₂N₃F₈P₃AgAu₃O₇ (%): C, 37.92; H, 3.18; N, 2.21. Found: C, 37.52; H, 3.31; N, 2.44. ESI-MS (MeCN): [O(AuPC₂₀H₂₀O₂N)₃Ag]²⁺, *m/z* = 863.58 (100%); [O(AuPC₂₀H₂₀O₂N)₃AgBF₄]⁺, *m/z* = 1814.63 (5.4%).

2: [Au₆Ag₂(C)(L¹)₆](BF₄)₄. Redistilled Et₃N (25 μ L, 0.2 mmol) was added to a solution of compound **3** (380 mg, 0.2 mmol) in dry dichloromethane (6 mL) under a nitrogen atmosphere, followed by Me₃SiCHN₂ (100 μ L 2 M hexane solution, 0.2 mmol). After the solution was stirred in dark overnight, excess AgBF₄ (39 mg, in 0.5 mL MeOH, 0.2 mmol) was added. The resultant solution was further stirred for another hour before filtration. The filtrate was transferred to a tube, and diethyl ether was layered on it. After two weeks, yellow-green block crystals (219 mg 58.0%) formed on the glass wall. ¹H NMR (500.2 MHz, CD₃CN, ppm): δ 7.82 (d, *J*_{H-H} = 7.5 Hz, *H* = 6, 4-py), 7.60 (s, *H* = 6, 6-py) 7.45–7.52 (m, *H* = 18, 3-py+*p*-Ph), 7.42 (t, *J*_{H-H} = 7.5 Hz, *H* = 24, *o*-Ph), 7.19 (t, *J*_{H-H} = 7.5 Hz, *H* = 24, *m*-Ph), 5.03 (s, *H* = 6, CH(OMe)₂), 3.11 (s, *H* = 6, -OMe). ¹³C NMR (125.8 MHz, CD₃CN, ppm): δ 154.30 (d, *J*_{C-P} = 83.0 Hz), 150.22 (d, *J*_{C-P} = 20.1 Hz), 138.00, 137.61, 134.19 (d, *J*_{C-P} = 15.1 Hz), 133.02, 130.88 (d, *J*_{C-P} = 11.3 Hz), 129.86 (d, *J*_{C-P} = 11.3 Hz), 126.22 (d, *J*_{C-P} = 55.3 Hz), 99.90, 52.80. ³¹P NMR (202.5 MHz, CD₃CN, ppm): δ 32.61 (s). Anal. Calcd. for C₁₂₁H₁₂₀B₄N₆F₁₆P₆Ag₂Au₆O₁₂·2CH₂Cl₂ (%): C, 37.39; H, 3.16; N, 2.13. Found: C, 37.39; H, 3.16; N, 2.18. ESI-MS (MeCN): [C(AuPC₂₀H₂₀O₂N)₆Ag]⁴⁺, *m/z* = 858.38 (58.9%); [C(AuPC₂₀H₂₀O₂N)₆Ag]³⁺, *m/z* = 1108.10 (100%); [C(AuPC₂₀H₂₀O₂N)₆Ag₂BF₄]³⁺, *m/z* = 1173.74 (57.1%); [C(AuPC₂₀H₂₀O₂N)₆AgBF₄]²⁺, *m/z* = 1706.98 (16.7%); [C(AuPC₂₀H₂₀O₂N)₆(AgBF₄)₂]²⁺, *m/z* = 1804.19 (6.9%).

1: [Au₆Ag₂(C)(L²)₆](BF₄)₄. To a flask containing **2** (200 mg, 52.9 mmol) was added 1 mL of trifluoroacetic acid. The solution was stirred at room temperature for 24 h, then diluted with 1 mL of dichloromethane and filtrated. The filtrate was added into a thin tube, and diethyl ether was layered on it. Green-yellow crystals (183 mg) were obtained after about 1 week. Yield: 98.5%. ¹H NMR (500.2 MHz, CD₃CN, ppm): δ 9.67 (s, *H* = 6, -CHO), 8.17 (s, *H* = 6, 6-py), 8.13 (d, *J*_{H-H} = 6.5 Hz, *H* = 6, 4-py), 7.51 (t, *J*_{H-H} = 8.0 Hz, *H* = 24, *o*-Ph), 7.48 (d, *J*_{H-H} = 3.0, *H* = 6, 3-py), 7.39 (t, *J*_{H-H} = 9.0 Hz, *H* = 12, *p*-Ph), 7.15 (t, *J*_{H-H} = 9.0 Hz, *H* = 24, *m*-Ph). ¹³C NMR (125.8 MHz, CD₃CN, ppm): δ 189.94, 159.02 (d, *J*_{C-P} = 84.3 Hz), 153.24, 138.87, 134.60 (d, *J*_{C-P} = 14.6 Hz), 133.39, 132.40, 131.28 (d, *J*_{C-P} = 15.1 Hz), 129.97 (d, *J*_{C-P} = 11.8 Hz), 125.80 (d, 64.7 Hz). ³¹P NMR (202.5 MHz, CD₃CN, ppm): δ 32.90 (s). Anal. Calcd. for C₁₀₉H₈₄B₄N₆F₁₆P₆Ag₂Au₆O₆ (%): C, 37.36; H, 2.42; N, 2.40. Found: C, 37.27; H, 2.31; N, 2.46. IR (KBr, cm⁻¹): ν 1706.8 (C=O, sharp). ESI-MS (MeCN): [C(AuPC₁₈H₁₄NO)₆Ag]⁴⁺, *m/z* = 789.29 (18.3%); [C(AuPC₁₈H₁₄NO)₆Ag]³⁺, *m/z* = 1016.44 (100%); [C(AuPC₁₈H₁₄NO)₆Ag₂BF₄]³⁺, *m/z* = 1081.08 (2.1.2%); [C(AuPC₁₈H₁₄NO)₆AgBF₄]²⁺, *m/z* = 1568.17 (11.6%); [C(AuPC₁₈H₁₄NO)₆(AgBF₄)₂]²⁺, *m/z* = 1678.19 (10.5%).

4a and 4b: [Au₆Ag₂(C)(L³)₆](BF₄)₄. **1** (15.0 mg, 4.28 mmol) was dissolved with 3 mL of MeCN, and (*S* or *R*)-1-phenylethylamine (3.3 μ L, 25.8 mmol) was injected. The mixture was stirred at room temperature for 24 h. Then all solvent was removed under vacuum and redissolved in 2 mL of dichloromethane. The clear red solution was filtrated into a thin tube, and diethyl ether was added. Red block-like crystals (13.1 mg) were obtained after about 1 week. Yield: ca.76.0%. ¹H NMR (500.2 MHz, CD₃CN, ppm): δ 8.16 (d, *J*_{H-H} = 6.5 Hz, *H* = 6, 4-py), 8.11 (s, *H* = 6, -CHN), 8.05 (s, *H* = 6, 6-py), 7.60–7.75 (broad, *H* = 96), 4.53 (q, *J*_{H-H} = 6.5 Hz, *H* = 6, C*H), 1.42 (d, *J*_{H-H} = 6.5 Hz, *H* = 18, -CH₃). ¹³C NMR (125.8 MHz, CD₃CN, ppm): δ 155.05, 155.05 (d, *J*_{C-P} = 83.0 Hz), 151.86 (d, *J*_{C-P} = 16.4 Hz), 144.68,

137.79, 134.35 (broad), 133.19, 133.11, 130.86 (d, $J_{C-P} = 16.4$ Hz), 129.84 (broad), 128.50, 127.16, 126.44, 125.68 (d, 52.8 Hz), 69.56, 24.06. ^{31}P NMR (202.5 MHz, CD_3CN , ppm): δ 32.87 (s). Anal. Calcd. for $\text{C}_{157}\text{H}_{138}\text{B}_4\text{N}_{12}\text{F}_{16}\text{P}_6\text{Ag}_2\text{Au}_6$ (%): C, 45.73; H, 3.37; N, 4.08. Found: C, 45.44; H, 3.86; N, 4.05. IR (KBr, cm^{-1}): ν 1638.3 (C = N, br.). ESI-MS (MeCN): $[\text{C}(\text{AuPC}_{26}\text{H}_{23}\text{N}_2)_6\text{Ag}_2]^{4+}$, $m/z = 943.84$ (34.4%); $[\text{C}(\text{AuPC}_{26}\text{H}_{23}\text{N}_2)_5(\text{AuPC}_{18}\text{H}_{14}\text{NO})\text{Ag}]^{3+}$, $m/z = 1188.16$ (58.4%); $[\text{C}(\text{AuPC}_{26}\text{H}_{23}\text{N}_2)_6\text{Ag}]^{3+}$, $m/z = 1222.55$ (100%); $[\text{C}(\text{AuPC}_{26}\text{H}_{23}\text{N}_2)_6\text{AgBF}_4]^{2+}$, $m/z = 1879.38$ (8.5%). Optical rotation of **4a** $[\alpha]_{\text{D}}^{26} = 26.6$ (CH_2Cl_2), **4b** $[\alpha]_{\text{D}}^{26} = -26.9$ (CH_2Cl_2).

5: $[\text{Au}_6\text{Ag}_2(\text{C}(\text{L}^4)_6(\text{BF}_4)_4)_2]$. **5** was prepared in the same process as for **4**. Six equivalent aniline was used instead of 1-phenylethylamine. Yellow crystals were obtained after about 2 weeks. Yield: ca.50%. ^1H NMR (500.2 MHz, CD_3CN , ppm): δ 8.27 (broad, $H = 18$, 4-py+6-py + -CHN), 7.57 (t, $J_{\text{H-H}} = 6.5$ Hz, $H = 24$, o-Ph), 7.49 (d, $J_{\text{H-H}} = 8.0$ Hz, $H = 6$, 3-py), 7.37–6.46 (m, $H = 24$, p-Ph+o-Ph(aniline)), 7.33 (t, $J_{\text{H-H}} = 7.5$ Hz, $H = 6$, p-Ph (aniline)), 7.12–7.28 (broad, $H = 36$, m-Ph +m-Ph(aniline)). ^{13}C NMR (125.8 MHz, CD_3CN , ppm): δ 155.35, 152.58 (broad), 150.15, 137.72, 134.47 (d, $J_{C-P} = 13.8$ Hz), 133.23, 130.87 (broad), 129.87 (d, $J_{C-P} = 10.1$ Hz), 129.45, 129.03, 128.24, 127.55, 126.39 (broad), 121.09. ^{31}P NMR (202.5 MHz, CD_3CN , ppm): δ 32.95 (s, broad). Anal. Calcd. for $\text{C}_{145}\text{H}_{116}\text{B}_4\text{N}_{12}\text{F}_{16}\text{P}_6\text{Ag}_2\text{Au}_6$ (%): C, 44.01; H, 2.95; N, 4.25. Found: C, 43.79; H, 3.46; N, 4.41. FT-ICR-MS (MeCN) calculated for $[\text{C}(\text{AuPC}_{24}\text{H}_{19}\text{N}_2)_6\text{Ag}_2]^{4+}$, $m/z = 901.8457$, found: $m/z = 901.857$; $[\text{C}(\text{AuPC}_{24}\text{H}_{19}\text{N}_2)_6\text{Ag}]^{3+}$, $m/z = 1166.492$, found: $m/z = 1166.4939$; $[\text{C}(\text{AuPC}_{24}\text{H}_{19}\text{N}_2)_6]^{2+}$, $m/z = 1695.786$, found: $m/z = 1695.767$.

Chirality Inversion. A total of 3.1 mg of **4b** (0.75 mmol) was dissolved in 5 mL of MeCN, and 5.8 μL of S-1-phenylethylamine (45.1 mmol, 10-fold excess) was added. The mixture was stirred at room temperature for 24 h. Then 50 μL of the sample solution was diluted to 3 mL, which was used for CD measurement.

In Situ Chiral Sensing of 1-Phenylethylamine. Typically, six equivalents of chiral 1-phenylethylamine were added to 3 mL of MeCN solution of **1** (4.76×10^{-4} M). The mixture was stirred at room temperature for 90 min, then the solution was diluted to 1.54×10^{-5} M for CD measurement.

■ ASSOCIATED CONTENT

Supporting Information

Physical measurements and characterization details. This material is available free of charge via the Internet at <http://pubs.acs.org>.

■ AUTHOR INFORMATION

Corresponding Author

qmwang@xmu.edu.cn

Notes

The authors declare no competing financial interest.

■ ACKNOWLEDGMENTS

This work is dedicated to Professor James Trotter in celebration of his 80th birthday. This work was supported by the Natural Science Foundation of China (21125102 and 21021061).

■ REFERENCES

- Schmidbaur, H.; Schier, A. *Chem. Soc. Rev.* **2012**, *41*, 370–412.
- Sculfort, S.; Braunstein, P. *Chem. Soc. Rev.* **2011**, *40*, 2741–2760.
- Adams, R. D.; Captain, B. *Acc. Chem. Res.* **2009**, *42*, 409–418.
- Selby, H. D.; Roland, B. K.; Zheng, Z. *Acc. Chem. Res.* **2003**, *36*, 933–944.
- Ford, P. C.; Cariati, E.; Bourassa, J. *Chem. Rev.* **1999**, *99*, 3625–3647.
- Templeton, A. C.; Wuelfing, W. P.; Murray, R. W. *Acc. Chem. Res.* **2000**, *33*, 27–36.

(7) Jia, J.-H.; Wang, Q.-M. *J. Am. Chem. Soc.* **2009**, *131*, 16634–16635.

(8) Qian, H.; Jiang, D.; Li, G.; Gayathri, C.; Das, A.; Gil, R. R.; Jin, R. *J. Am. Chem. Soc.* **2012**, *134*, 16159–16162.

(9) Zhu, M.; Aikens, C. M.; Hendrich, M. P.; Gupta, R.; Qian, H.; Schatz, G. C.; Jin, R. *J. Am. Chem. Soc.* **2009**, *131*, 2490–2492.

(10) Ingram, R. S.; Hostetler, M. J.; Murray, R. W. *J. Am. Chem. Soc.* **1997**, *119*, 9175–9178.

(11) Templeton, A. C.; Hostetler, M. J.; Warmoth, E. K.; Chen, S.; Hartshorn, C. M.; Krishnamurthy, V. M.; Forbes, M. D. E.; Murray, R. W. *J. Am. Chem. Soc.* **1998**, *120*, 4845–4849.

(12) Schmid, G.; Bäuml, M.; Beyer, N. *Angew. Chem., Int. Ed.* **2000**, *39*, 181–183.

(13) Konppe, S.; Azoulay, R.; Dass, A.; Bürgi, T. *J. Am. Chem. Soc.* **2012**, *134*, 20302–20305.

(14) Shibu, E. S.; Muhammed, M. A. H.; Tsukuda, T.; Pradeep, T. *J. Phys. Chem. C.* **2008**, *112*, 12168–12176.

(15) Cohen, S. M. *Chem. Rev.* **2012**, *112*, 970–1000.

(16) Cohen, S. M. *Chem. Sci.* **2010**, *1*, 32–36.

(17) Tanabe, K. K.; Cohen, S. M. *Chem. Soc. Rev.* **2011**, *40*, 498–519.

(18) Zhao, D.; Tan, S.; Yuan, D.; Lu, W.; Rezenom, Y. H.; Jiang, H.; Wang, L.; Zhou, H.-C. *Adv. Mater.* **2011**, *23*, 90–93.

(19) Chakrabarty, R.; Stand, P. J. *J. Am. Chem. Soc.* **2012**, *134*, 14738–14741.

(20) Wang, M.; Lan, W.-J.; Zheng, Y.-R.; Cook, T. R.; White, H. S.; Stang, P. T. *J. Am. Chem. Soc.* **2011**, *133*, 10752–10755.

(21) Belowich, M. E.; Stoddart, J. F. *Chem. Soc. Rev.* **2012**, *41*, 2003–2024.

(22) Corbett, P. T.; Leclaire, J.; Vial, L.; West, K. R.; Wietor, J.-L.; Sanders, J. K. M.; Otto, S. *Chem. Rev.* **2006**, *106*, 3652–3711.

(23) Wolf, C.; Bentley, K. W. *Chem. Soc. Rev.* **2013**, *42*, 5408–5424.

(24) Jia, J.-H.; Liang, J.-X.; Lei, Z.; Cao, Z.-X.; Wang, Q.-M. *Chem. Commun.* **2011**, *47*, 4739–4741.

(25) Dry, E. F. V.; Clegg, J. K.; Breiner, B.; Whitaker, D. E.; Stefak, R.; Nitschke, J. R. *Chem. Commun.* **2011**, *47*, 6021–6023.

(26) (a) Crystal data for **1**: $6\text{CH}_2\text{Cl}_2$: $\text{C}_{105}\text{H}_{84}\text{B}_4\text{N}_6\text{O}_6\text{F}_{16}\text{P}_6\text{Ag}_2\text{Au}_6$, $6\text{CH}_2\text{Cl}_2$, $a = 15.8230(11)$, $b = 15.9244(10)$, $c = 16.5291(13)$ Å, $\alpha = 67.867(7)^\circ$, $\beta = 61.943(7)^\circ$, $\gamma = 72.387(6)^\circ$, $V = 3364.3(4)$ Å³, triclinic space group P-1, $Z = 1$, $T = 100(2)$ K, 25527 reflections measured, 11822 unique ($R_{\text{int}} = 0.0453$), final $R_1 = 0.0520$, $wR_2 = 0.1329$ for 9134 observed reflections [$I > 2\sigma(I)$]. (b) Crystal data for **2**: $2\text{CH}_2\text{Cl}_2$: $\text{C}_{121}\text{H}_{120}\text{B}_4\text{N}_6\text{O}_{12}\text{F}_{16}\text{P}_6\text{Ag}_2\text{Au}_6$, $2\text{CH}_2\text{Cl}_2$, $a = 15.3322(11)$, $b = 15.4373(9)$, $c = 16.4557(11)$ Å, $\alpha = 82.767(5)^\circ$, $\beta = 64.786(7)^\circ$, $\gamma = 73.405(6)^\circ$, $V = 3377.0(4)$ Å³, triclinic space group P-1, $Z = 1$, $T = 100(2)$ K, 21470 reflections measured, 11862 unique ($R_{\text{int}} = 0.0540$), final $R_1 = 0.0594$, $wR_2 = 0.1526$ for 8704 observed reflections [$I > 2\sigma(I)$]. (c) Crystal data for **3**: $\text{C}_{120}\text{H}_{120}\text{B}_4\text{N}_6\text{O}_{14}\text{F}_{16}\text{P}_6\text{Ag}_2\text{Au}_6$, $a = 13.9185(10)$, $b = 14.5434(18)$, $c = 18.3354(18)$ Å, $\alpha = 106.857(10)^\circ$, $\beta = 94.398(7)^\circ$, $\gamma = 115.063(10)^\circ$, $V = 3131.2(5)$ Å³, triclinic space group P-1, $Z = 1$, $T = 100(2)$ K, 19808 reflections measured, 11014 unique ($R_{\text{int}} = 0.0764$), final $R_1 = 0.0599$, $wR_2 = 0.1133$ for 7469 observed reflections [$I > 2\sigma(I)$]. (d) Crystal data for **4a**: $\text{C}_{157}\text{H}_{138}\text{B}_4\text{N}_{12}\text{F}_{16}\text{P}_6\text{Ag}_2\text{Au}_6$, $a = 21.5456(7)$, $b = 21.5456(7)$, $c = 68.438(2)$ Å, $\gamma = 120^\circ$, $V = 27513.4(15)$ Å³, trigonal space group R32, $Z = 6$, $T = 100(2)$ K, 32892 reflections measured, 11120 unique ($R_{\text{int}} = 0.0534$), final $R_1 = 0.0840$, $wR_2 = 0.2254$ for 7337 observed reflections [$I > 2\sigma(I)$]. Flack factor = $-0.02(3)$. (e) Crystal data for **4b**: $\text{C}_{157}\text{H}_{138}\text{B}_4\text{N}_{12}\text{F}_{16}\text{P}_6\text{Ag}_2\text{Au}_6$, $a = 21.5216(14)$, $b = 21.5216(14)$, $c = 68.567(4)$ Å, $\gamma = 120^\circ$, $V = 27504(3)$ Å³, trigonal space group R32, $Z = 6$, $T = 100(2)$ K, 33350 reflections measured, 11920 unique ($R_{\text{int}} = 0.0594$), final $R_1 = 0.0901$, $wR_2 = 0.2504$ for 9282 observed reflections [$I > 2\sigma(I)$]. Flack factor = $-0.01(3)$. (f) Crystal data for **5**: $4\text{CH}_2\text{Cl}_2 \cdot 2\text{H}_2\text{O}$: $\text{C}_{145}\text{H}_{116}\text{B}_4\text{N}_{12}\text{F}_{16}\text{P}_6\text{Ag}_2\text{Au}_6 \cdot 4\text{CH}_2\text{Cl}_2 \cdot 2\text{H}_2\text{O}$, $a = 14.9418(3)$, $b = 18.9928(4)$, $c = 28.0858(5)$ Å, $\beta = 92.507(2)^\circ$, $V = 7962.7(3)$ Å³, monoclinic space group $P2(1)/n$, $Z = 2$, $T = 100(2)$ K, 30097 reflections measured, 15659 unique ($R_{\text{int}} = 0.0348$), final $R_1 = 0.0550$, $wR_2 = 0.1602$ for 12697 observed reflections [$I > 2\sigma(I)$].

(27) Dragana, J. M.; Pescitelli, G.; Tran, L.; Lynch, V. M.; Anslyn, E. V.; Bari, L. D. *J. Am. Chem. Soc.* **2012**, *134*, 4398–4407.

- (28) Joyce, L. A.; Maynor, M. S.; Dragna, J. M.; Cruz, G. M.; Lynch, V. M.; Canary, J. W.; Anslyn, E. V. *J. Am. Chem. Soc.* **2011**, *133*, 13746–13752.
- (29) You, L.; Berman, J. S.; Anslyn, E. V. *Nat. Chem.* **2011**, *3*, 943–948.
- (30) Castagnetto, J. M.; Xu, X.; Berova, N. D.; Canary, J. W. *Chirality* **1997**, *9*, 616–622.
- (31) Provorse, M. R.; Aikens, C. M. *J. Am. Chem. Soc.* **2010**, *132*, 1302–1310.
- (32) Laguna, A. et al. *Modern Supramolecular Gold Chemistry*; Wiley-VCH: Germany, 2008.
- (33) Norguez, C.; Garzón, I. L. *Chem. Soc. Rev.* **2009**, *38*, 757–771.
- (34) Ziegler, M.; Zelewsky, A. *Coord. Chem. Rev.* **1998**, *177*, 257–300.
- (35) Mason, S. F. *Molecular Optical Activity and the Chiral Discriminations*; Cambridge University Press: Cambridge, U.K., 1982.
- (36) Bosnich, B. *Acc. Chem. Res.* **1969**, *2*, 266–273.
- (37) Telfer, S. G.; Tajima, N.; Kuroda, R. *J. Am. Chem. Soc.* **2004**, *126*, 1408–1418.
- (38) Telfer, S. G.; Kuroda, R.; Sato, T. *Chem. Commun.* **2003**, 1064–1065.
- (39) Wärnmark, K.; Baxter, P. N. W.; Lehn, J.-M. *Chem. Commun.* **1998**, 993–994.
- (40) Gautier, C.; Bürgi, T. *J. Am. Chem. Soc.* **2008**, *130*, 7077–7084.
- (41) Farina, V.; Reeves, J. T.; Senanayake, C. H.; Song, J. J. *Chem. Rev.* **2006**, *106*, 2734–2793.
- (42) France, S.; Guerin, D. J.; Miller, S. J.; Lectka, T. *Chem. Rev.* **2003**, *103*, 2985–3012.
- (43) Berova, N.; Bari, L. D.; Pescitelli, G. *Chem. Soc. Rev.* **2007**, *36*, 914–931.
- (44) Pescitelli, G.; Bari, L. D.; Berova, N. *Chem. Soc. Rev.* **2011**, *40*, 4603–4625.
- (45) Iwaniuk, D. P.; Wolf, C. *J. Am. Chem. Soc.* **2011**, *133*, 2414–2417.